Pulsed Nuclear Magnetic Resonance of Ne^{21} in Solid and Liquid Neon*†

Rodney Henry‡ and R. E. Norberg
Department of Physics, Washington University, St. Louis, Missouri 63130
(Received 13 April 1972)

Pulsed nuclear-magnetic-resonance (NMR) measurements have been performed on isotopically enriched Ne^{21} in solid and liquid neon. Data presented include spin-spin relaxation times (T_2) in solid neon and spin-lattice relaxation times (T_1) in the solid and liquid. It is concluded that quadrupolar processes dominate the Ne^{21} nuclear spin-lattice relaxation in both the solid and the liquid. Coefficients of atomic self-diffusion are determined, with the results (solid) $D = (0.12^{+0.15}_{-0.05})\, e^{-(947\pm38)/RT}$ cm^2/sec and (liquid) $D = (6.6^{+2.1}_{-1.6}) \times 10^{-4} e^{-(211\pm15)/RT}$ cm^2/sec.

I. INTRODUCTION

Solid and liquid neon have been the subject of relatively fewer reported experimental and theoretical investigations than have the condensed phases of some other rare gases. Neon is, however, particularly interesting because of its relatively light atomic mass and corresponding semiclassical behavior.

In the present work, Ne^{21} spin echoes and free-induction decays have been used to determine spin-spin relaxation times (T_2) and spin-lattice relaxation times (T_1) in solid and liquid neon. Ne^{21} has spin $\frac{3}{2}$, and nuclear quadrupolar interactions provide most of the spin-lattice relaxation. It is proposed that anharmonic effects are important in the relaxation and that atomic vibrations may contribute appreciably to T_1 in the liquid near the triple point. Coefficients of atomic self-diffusion are determined, and the solid diffusion is found to display an activation energy consistent with those for other rare-gas solids, when compared via a quantum-mechanical law of corresponding states. Attempts to determine shifts of the Ne^{21} resonance showed no shifts as large as 2 ppm.

II. EXPERIMENTAL PROCEDURE

Ne^{21} nuclear spin echoes and free-induction decays were observed with a gated coherent NMR spectrometer operating at a frequency of 3 MHz and a dc magnetic field of 8920 G. The spectrometer, previously described by Warren,[1] produced pulsed rf fields of 20 G. The pulses adequately covered the resonance line, since the Ne^{21} rigid-lattice linewidth in our solid-neon samples was found to be 0.41 G. The 8920-G field, produced by an electromagnet, was controlled to within 10 ppm/h by a Hall probe regulator. Spin-spin relaxation times were measured from free-induction decays and from spin-echo envelopes. Spin-lattice relaxation times were measured by observing the free-induction decay following a saturating pulse τ-90° sequence.

A search was made for resonant field shifts over the solid-liquid temperature interval from 23 to 34 K, but none were observed and the corresponding shifts were less than 0.010 in 8920 G.

The samples consisted of about 250 cm^3 (STP) of neon isotopically enriched to 51 at.% Ne^{21} (normal abundance 0.26 at.%). The enriched samples, which were obtained from the Mound Laboratories, contained no magnetic nuclei other than Ne^{21} in any measurable degree. The normal boiling point of natural-abundance neon is 27.07 K and the triple point is 24.56 K.[2] For our isotopically enriched samples these transitions would be expected to occur at a temperature higher by about 0.05 K. Neon solidifies in a cubic close-packed lattice with a cube-edge lattice parameter (at 4.25 K) of 4.464 Å.[3]

Control of the sample temperature was particularly important, since the solid NMR line was observed to narrow by a factor of 3000 over the 10-deg interval between 14 K and the triple point. The neon sample was condensed into a nylon sample container which was connected to a copper block. The block was in good thermal contact with a single-shot refrigerator. Temperatures were controlled by regulating the vapor pressure of the liquid in the probe refrigerator with a Cartesian manostat. The outer wall of the can containing the refrigerator chamber and neon sample was cooled by liquid helium or by cold helium vapor. The fluid used in the single-shot refrigerator was neon, deuterium, or hydrogen, depending on the particular temperature interval of interest. Using this method of temperature control, we were able to control the temperature to within ±0.02 K for periods of several hours. The spatial temperature variation over the neon sample was estimated to be less than 0.02 K.

The polycrystalline neon samples were condensed via a 0.020-in.-diam stainless-steel capillary, 3 ft. long, with one end at room temperature and the other at 26 K. The 250-cm^2 (STP) neon sample was condensed over a 30-min interval.

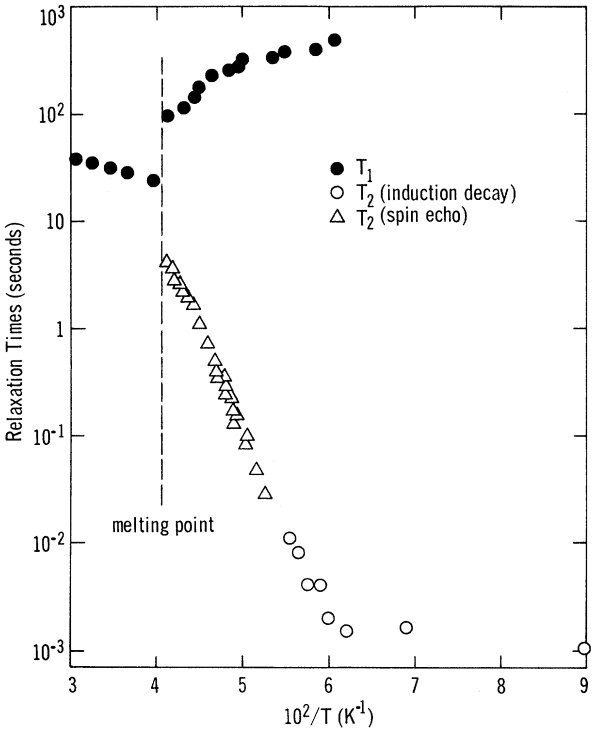

FIG. 1. Spin-spin and spin-lattice relaxation times for Ne^{21} in solid and liquid neon.

Because the gas flow through the capillary was slow, the capillary served as an efficient cold trap for oxygen. Since the vapor pressure of oxygen is about 10^{-12} Torr at 26 K,[4] the oxygen impurities in the condensed neon samples were probably less than 0.2 ppm.

III. SPIN-RELAXATION TIMES

The results of our measurements of Ne^{21} spin relaxation in neon are summarized in Fig. 1. The NMR line in the solid narrows (T_2 increases) above 14 K. The T_2 increase proceeds exponentially, as a function of reciprocal temperature, up to a value of 4 sec near the triple point. The spin-lattice relaxation time decreases as the temperature of the solid is increased. T_1 decreases abruptly at the melting point from about 90 sec in the solid to 23 sec in the liquid and increases with increasing temperature in liquid neon. The experimental difficulty of measuring spin-spin relaxation times of greater than 25 sec in the presence of appreciable diffusion prevented reliable determinations of T_2 in the liquid.

Below 17 K the free-induction decays could be well represented by a Gaussian function. Both spin-echo and free-induction decay data are presented in Fig. 1. Special care was taken in the T_2 determination at 11.1 K (shown in Fig. 2), which yielded a rigid-lattice Gaussian T_2 of 1.17 $\pm$0.07 msec, corresponding to a resonance half-width of 0.41 G and a second moment of 7.30×10^5 rad/sec^2. The measurement required waiting times of about 30 min between observations of the free-induction decay. The Van Vleck expression[5]

$$\sigma_D^2 = \tfrac{3}{5}\gamma^4 h^2 I(I+1) f \textstyle\sum_j r_{ij}^{-6}$$

for the rigid-lattice dipolar second moment of the resonance line in a powder sample yields, for our 51 at.% Ne^{21} sample, the calculated result $\sigma_D^2 = 3.51 \times 10^5$ rad^2/sec^2, which is less than one-half as large as the second moment observed.

Ne^{21} has spin $\frac{3}{2}$ and a substantial quadrupole moment. Electric field gradients arising from defects in the cubic crystalline lattice can produce a significant broadening of the Ne^{21} resonance. If there were a well-resolved quadrupole splitting in solid neon the central transition for spin $\frac{3}{2}$ would have a dipolar second moment reduced[6] from the Van Vleck value by as much as 20%, which would correspond to $T_2' = 1.73$ msec. The observed rigid-lattice value of $T_2 = 1.17$ msec suggests that there exists an unresolved quadrupolar broadening arising from random defects.

Additional support for the hypothesis of unresolved quadrupole broadenings, well covered by the rf pulse, is provided by the free-induction decays at the melting transition. The initial amplitudes of the decays on either side of the melting transition were found to be the same to within $\pm$3%. Also, compound envelopes were observed for the decay of the spin echoes in solid neon above 20 K. An initially rapid decay was followed

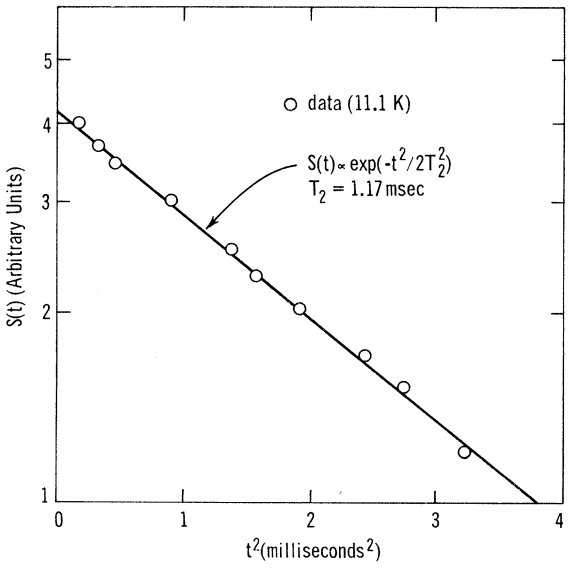

FIG. 2. Ne^{21} free-induction decay in solid neon at 11.1 K ($\ln S$ vs t^2).

by a slower exponential decay of the echo amplitudes. Above 19 K, spin echoes from a 90°–180° two-pulse sequence were used to measure T_2 in the solid. The long spin-lattice relaxation times made it difficult to use more complicated pulse sequences. The slower exponential decay of the echo envelope will be interpreted in Sec. IV to reflect the spin-spin relaxation associated with the motionally narrowed dipolar broadening of the central $-\frac{1}{2} \leftrightarrow \frac{1}{2}$ transition.

The Ne^{21} resonance characteristics described above for solid neon differ considerably from those observed[7] for Xe^{131} in solid xenon. In the xenon case melting was accompanied by a factor-of-$\frac{5}{2}$ increase in the initial amplitude of the induction decays, and the decays in the rigid lattice were found to be distinctly non-Gaussian. The Xe^{131} data were interpreted as reflecting a second-order quadrupole broadening of the central $-\frac{1}{2} \leftrightarrow \frac{1}{2}$ transition.

IV. SELF-DIFFUSION IN SOLID NEON

The T_2 increase shown in Fig. 1 above 14 K corresponds to motional narrowing in the adiabatic limit. T_1 remains much larger than T_2 throughout the temperature range of the solid and the correlation frequency for atomic motion turns out to be much smaller than the 3-MHz resonance frequency. In the adiabatic limit ($\omega_0 \tau_c \gg 1$) Kubo and Tomita[8] have derived the expression

$$\left(\frac{1}{T_2}\right)^2 = \frac{4 \ln 2}{\pi} \sigma^2 \tan^{-1}\left(\frac{\pi \tau_c}{(4 \ln 2) T_2}\right), \tag{1}$$

in which T_2 is the reciprocal of the half-width at half-maximum of the motionally narrowed Lorentzian resonance line. For the well-narrowed line ($\tau_c \sigma \ll 1$), Eq. (1) reduces to the Anderson-Weiss[9] expression

$$1/T_2 = \sigma^2 \tau_c \, . \tag{2}$$

For an fcc lattice, τ_c is related to the coefficient of atomic self-diffusion by the expression

$$\tau_c = d^2/12D \, , \tag{3}$$

where d is the cube-edge lattice parameter and D is the coefficient of self-diffusion. If there are not correlations between successive jumps of the atoms, or if the degree of correlation is known,[10] values of D can be determined from measurements of T_2.

Figure 3 presents, on an expanded scale, the spin-echo T_2 data for Ne^{21} in solid neon above 19 K. The data exhibit an exponential variation with $1/T$ between 19 and 23 K, so it appears that the coefficient of self-diffusion in that temperature range in solid neon can be represented by an Arrhenius relation

$$D = D_0 e^{-E_D/RT} \, , \tag{4}$$

where E_D is the activation energy for atomic self-diffusion.

The T_2 data in Fig. 3 were obtained from analysis of the slower exponential decay of the compound envelope of spin echoes in a 90°–180° two-pulse experiment. Thus, the data are interpreted as reflecting the dipolar-broadened central $-\frac{1}{2} \leftrightarrow \frac{1}{2}$ transition. Abragam[11] has pointed out that the dipolar second moment of the central $-\frac{1}{2}$ to $\frac{1}{2}$ transition for spins $\frac{3}{2}$ having different quadrupole couplings with random defects is $\frac{9}{10}$ of that obtained in the absence of quadrupole interactions. To calculate diffusion parameters from the T_2 data and Eqs. (2) and (4) we have used a coefficient of 0.85 as a compromise between the "like" spin coefficient $\frac{4}{5}$ and the "semilike" spin coefficient $\frac{9}{10}$.[11] This corresponds to $(\sigma_D^2)' = 2.97 \times 10^5$ rad^2/sec^2 and diffusion parameters

$$D_0 = 0.12 \, ^{+0.15}_{-0.05} \text{ cm}^2/\text{sec} \, ,$$

$$E_D = 947 \pm 38 \text{ cal/mole} \, .$$

Table I summarizes the diffusion coefficients which have been reported for rare-gas solids. The

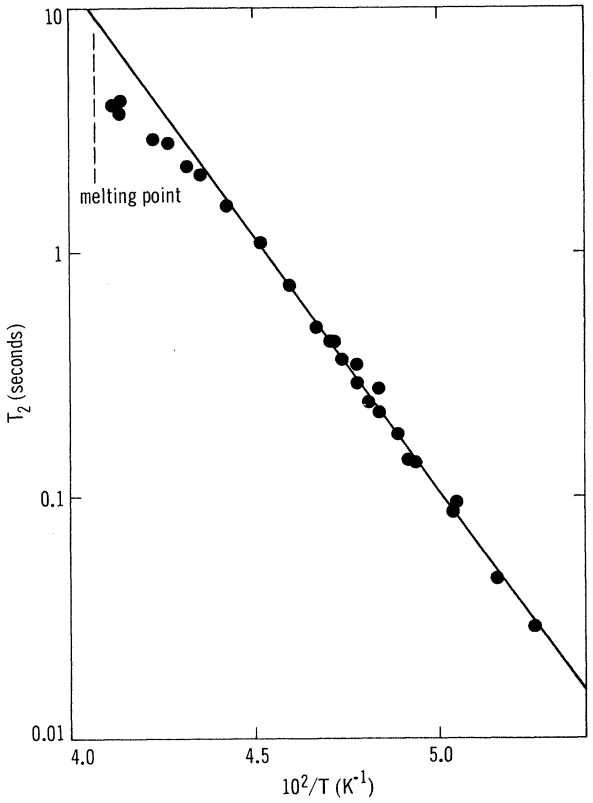

FIG. 3. Spin-spin relaxation times determined from spin echoes in solid neon. The solid line is a least-squares fit between 23 and 19 K.

TABLE I. Coefficients of atomic self-diffusion for rare-gas solids.

	D_0 (cm^2/sec)	E_D (cal/mole)		$2L_0$ (cal/mole)
Ne	$0.12^{+0.15}_{-0.05}$	947 ± 38	(NMR)	896 [a]
Ar	$0.20^{+0.35}_{-0.14}$ [b]	3600 ± 150 [b]	(tracer)	3716 [a]
Kr	3^{+4}_{-2}	4800 ± 200 [c]	(tracer)	5332 [a]
		(5250) [d]	(NMR)	
Xe	$7.3^{+0.4}_{-0.2}$ [e]	7400 ± 50 [e]	(NMR)	7656 [a]

[a]Reference 2. [The heat of sublimation for argon (Ref. 16) has been corrected to 1858 cal/mole, J. A. Morrison (private communication).]
[b]Reference 13.
[c]Reference 14.
[d]Reference 15.
[e]Reference 12.

data for neon and xenon[12] are from NMR measurements, while those for argon[13] and krypton[14] are from radioactive tracer measurements. Also included is an NMR result for krypton estimated from the onset of motional narrowing.[15] It has been pointed out[12] that the activation energies for self-diffusion measured in solid argon and xenon are nearly equal to twice the lattice sublimation energies. As Table I indicates, this correspondence also holds true for neon and krypton. Thus, E_D in rare-gas solids is nearly the same as the work required to remove a single atom from the lattice to infinity.

The application of the law of corresponding states to an examination of the properties of neon presents the interesting question of the effects of an appreciable deviation from classical behavior. Table II summarizes a set of molecular parameters ϵ and σ appropriate for a Lennard-Jones (6-12) interatomic two-body potential and the deBoer quantum parameter $[\Lambda^* = h/\sigma(me)^{1/2}]$ for the rare gases.[17]

According to the classical law of corresponding states,[2,18] the lattice cohesive energies and the activation energies for self-diffusion have the reduced forms $L_0^* = L_0/\epsilon$ and $E_D^* = E_D/\epsilon$, respectively. As Table II indicates, E_D^* and $2L_0$ vary by less than 10% among Ar, Kr, and Xe but are some 20% smaller in Ne.

Bernardes[19] has applied a quantum-mechanical law of corresponding states to the description of the effects of zero-point motion on the properties of rare-gas solids. His results include a variation, with the deBoer quantum parameter of the reduced lattice cohesive energies, according to the approximate expression

$$L_0^* = L_{00}^*(1 - 0.601\Lambda^* + 0.203\Lambda^{*2}) , \quad (5)$$

where $L_{00}^* = 8.61$ is the classical reduced cohesive energy for a close-packed solid having no zero-point energy. Table II includes the quantities $E_D^*/2L_{00}^*$ and L_0^*/L_{00}^*, which also are plotted as a function of Λ^* in Fig. 4 (which corresponds to Fig. 2 in Bernardes's paper[19]). The line indicated in Fig. 4 corresponds to Eq. (5) and one sees that Bernardes's quantum-mechanical modification of the law of corresponding states accounts very well for the variation of the observed diffusion activation energies among the rare-gas solids. The correspondence among the various data suggests that the activation energy reported by Chadwick and Morrison[14] for self-diffusion in solid krypton may be low by about 10%. Indeed, NMR measurements[15] on Kr^{83} in solid krypton indicate an agreement of the krypton T_2 data with an $E_D \simeq 5250$ cal/mole rather than with the tracer result[14] of 4800 cal/mole. The corresponding $E_0^*/2L_{00}^*$ from the krypton NMR experiments is 0.935, which also is shown in Fig. 4.

In summary, the activation energy observed for atomic self-diffusion in solid neon corresponds well with those activation energies reported for the other rare-gas solids, when the effect of zero-point motion is taken into consideration.

The coefficients of self-diffusion reported from NMR measurements in solid neon, krypton,[15] and xenon[12] have not included corrections for cor-

TABLE II. Comparison of reduced corresponding states parameters.

	ϵ (cal/mole)	σ (Å)	Λ^*	E_D^*	$E_D^*/2L_{00}^*$	$2L_0^*$	L_0^*/L_{00}^*
Ne	72.9	2.789 [a]	0.577 [a]	12.99 ± 0.5	0.754	12.29	0.713
Ar	238	3.403	0.186	15.13 ± 0.6 [b]	0.879	15.61	0.906
Kr	326	3.638	0.102	14.72 ± 0.7 [c]	0.855	16.36	0.950
				(16.10) [d]	(0.935)		
Xe	459	3.961	0.0635	16.12 ± 0.1 [e]	0.936	16.68	0.969

[a]Data in the first three columns are from Ref. 17. The last four columns are calculated from the data in Table I.
[b]Reference 13.
[c]Reference 14.
[d]Reference 15.
[e]Reference 12.

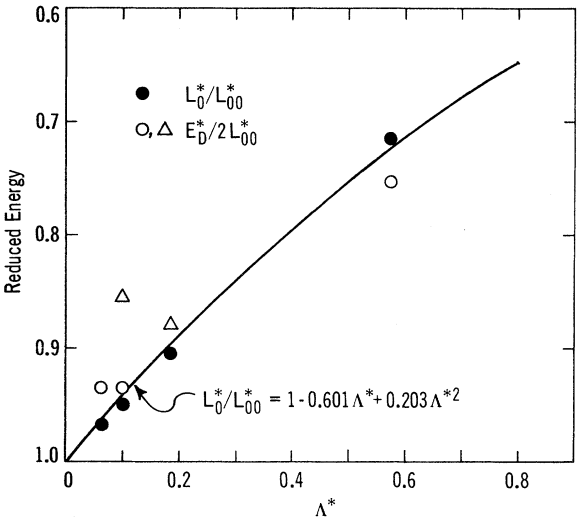

FIG. 4. Variation of reduced energies as a function of the deBoer quantum parameter Λ^*. The data of Table II are presented with reduced latent heats of sublimation (L_0^*/L_{00}^*) indicated by solid circles. The open circles indicate the reduced diffusion energies ($E_D^*/2L_{00}^*$) from NMR measurements and the triangles indicate ($E_D^*/2L_{00}^*$) from tracer measurements.

relation effects.[10,20] For a free vacancy diffusion mechanism and an fcc lattice, the correlation correction in the limit of adiabatic narrowing increases the deduced values of D by a factor of $(0.55)^{-1}$ or 1.82. The T_2 data in the rare-gas solids do not extend very far towards the high-temperature limit of extreme narrowing, where the correction would become $(0.67)^{-1}$. Consequently, the correlation correction does not produce appreciable reductions in the activation energies E_D reported for the rare-gas solids.

V. SPIN-LATTICE RELAXATION IN SOLID NEON

There are two probable mechanisms for nuclear spin-lattice relaxation of Ne^{21} in solid neon. One is the diffusion-modulated nuclear dipole-dipole interaction and the other is the interaction of the nuclear quadrupole moment with fluctuating electric field gradients.

A theory of nuclear dipolar relaxation associated with translational atomic diffusion in a crystalline lattice has been given by Torrey.[21] Torrey's result for the nuclear relaxation rate may be written

$$(1/T_{1D}) = \tfrac{8}{5}\pi\gamma^4\hbar^2 I(I+1)(n/k^3 l^3\omega)\,\phi(k,y)\ , \qquad (6)$$

where the notation is that of Resing and Torrey.[22] The neon diffusion coefficient determined from the T_2 data in Sec. IV can be used with Eq. (6) and the appropriate tabulated function ϕ to calculate the nuclear dipolar contribution to the Ne^{21} relaxation rate.

The solid-neon T_1 data shown in Fig. 1 were obtained for sample temperatures between 16.42 and 24.16 K. Neglecting the 1% variation of the neon fcc lattice parameter over this temperature range, Eq. (6) yields a dipolar T_{1D} proportional to D^{-1} and equal to 170 sec at 24.5 K.

The solid points in Fig. 5 present the experimental T_1 data for Ne^{21} in our solid-neon samples, plotted as $\ln T_1$ vs $1/T$. The straight line indicates the calculated T_{1D} result of Eq. (6). There are no adjustable parameters in the calculations of the dipolar T_{1D}, so it is of interest to examine the residual nondipolar relaxation rate $1/T_1'$ by subtracting the dipolar rate,

$$1/T_1' = 1/T_1 - 1/T_{1D}\ . \qquad (7)$$

In Fig. 5 this subtraction has been performed for the data near the melting point and the resulting T_1' data points are shown as open circles.

Van Kranendonk[23] has presented a theory of quadrupolar nuclear spin-lattice relaxation in a harmonic approximation and Van Kranendonk and Walker[24,25] have more recently proposed a theory of quadrupolar relaxation in anharmonic solids. The harmonic and anharmonic theories predict nearly the same temperature dependence for the quadrupolar relaxation rate,

$$1/T_{1Q} \propto T^{*2}E(T^*)\ , \qquad (8)$$

where $T^* = T/\Theta_D$ and the Van Kranendonk function $E(T^*)$ is independent of temperature for $T > \Theta_D$ and proportional to T^{*5} for $T \ll \Theta_D$. Taking $\Theta_D \simeq 65$ K for neon between 24.5 and 16.4 K, $E(T^*)$ varies between 0.69 and 0.45 in that range, and the temperature variation predicted by Eq. (8) deviates

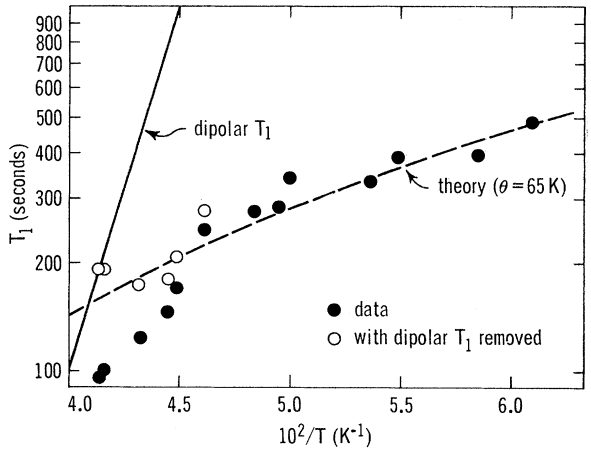

FIG. 5. Spin-lattice relaxation times for Ne^{21} in solid neon. The solid line indicates the calculated dipolar T_1 and the open circles show residual T_1 points after the dipolar T_1 contribution has been removed from the observed data. The dashed line shows the temperature dependence theoretically predicted for quadrupolar relaxation.

by about 30% from a T^2 dependence. The dashed line in Fig. 5 has been drawn with the temperature dependence of Eq. (8) and normalized to a magnitude of $T_{1Q} = 490$ sec at 16.4 K. Within the experimental uncertainties, the residual T_1' data show a temperature dependence in reasonable agreement with the quadrupolar relaxation described by Eq. (8), so we turn next to a consideration of the anticipated magnitudes of the quadrupolar relaxation rates.

Van Kranendonk[23] used a first-order Raman process to describe the harmonic contribution to the phonon-induced quadrupolar nuclear spin-lattice relaxation in alkali halides. The method subsequently has been applied[1,26] to a discussion of the relaxation of Xe^{131} in solid xenon. The quadrupolar contribution to the relaxation rate of a spin-$\frac{3}{2}$ nuclide is given by

$$1/T_1 = \tfrac{2}{5}(W_1 + 4W_2) , \tag{9}$$

where W_1 and W_2 refer to the $\Delta m = 1$ and $\Delta m = 2$ transitions. Using the notation of Warren and Norberg,[26] the transition probabilities computed for an fcc rare-gas solid in the Debye approximation are

$$W_{m,m+\mu} = C\,|Q_{\mu m}|^2\, T^{*2} \sum_{n=1}^{6} N_{\mu n} D_n(T^*) , \tag{10}$$

where $T^* = T/\Theta_D$ and $C = 3n_0/\pi v^3 d^2$. Here n_0 is the number of atoms per unit volume, v is the velocity of sound, and d is the mass density of the crystal. The functions $D_n(T^*)$ are determined by the lattice structure, and the gradient functions $N_{\mu n}$ depend upon the distribution of electronic charge about the nucleus.

The lattice functions are given by

$$D_n(T^*) = T^* \int_0^{1/T^*} [x^2 e^x/(e^x - 1)^2]\, L_n(cT^* x)\, dx , \tag{11}$$

where the L_n lattice functions are defined for an fcc lattice in Ref. 26.

For solid xenon,[26] the six functions $D_n(T^*)$ were evaluated in a high-temperature approximation and the gradient functions $N_{\mu n}$ were calculated on an overlap model of the crystalline electronic wave function. For the case of solid neon we have used the $N_{\mu n}$ given by Warren and Norberg[26] and have numerically evaluated the lattice functions $D_n(T^*)$ for the intermediate values of T^* appropriate for neon. The resulting temperature dependence for the neon quadrupolar T_1 is indicated by the dashed line in Fig. 5.

The electric field gradients in neon arise principally from the distortion of the electronic distribution by the attractive Van der Waals interaction. The gradients arising from exchange interactions are negligibly small in comparison. Following Adrian[27] one can calculate the Van der Waals gradient

$$V_{zz} = (3\alpha^2/8R^6)\langle V_{zz}\rangle_{2p} , \tag{12}$$

where $\alpha = 0.392\times10^{-24}$ cm^2 is the polarizability[28] of neon and $R = 3.21$ Å is the separation of neon atoms in the solid near the melting point. $\langle V_{zz}\rangle_{2p}$ is the field gradient at the neon nucleus produced by a $2p$ electron, which can be determined from the reported[29] neon hyperfine splitting of $b = 111.55$ MHz. $\langle V_{zz}\rangle_{2p} = 2\hbar b/eQ$ is then 3.30×10^{16} statC/cm^2 and $V_{zz} = 1.74\times10^{12}$ statC/cm^2.

The velocity of sound was estimated using a Θ_D of 65 K, with n_0 and d obtained from Ref. 2.

The corresponding T_{1Q} calculated at 24.56 K from the harmonic process is 1.4×10^5 sec, which is nearly three orders of magnitude larger than the experimental value (Fig. 5) of 150 sec observed in the solid at the melting point.

Van Kranendonk and Walker[24,25] have pointed out that an anharmonic Raman process probably plays a dominant role in the quadrupolar nuclear relaxation in ionic crystals. In these materials the observed T_1 values are smaller by factors between 100 and 800 than those predicted by the harmonic theory.

Anharmonicity should play an even more important role in the neon relaxation, but the spin-lattice coupling coefficients required for a calculation of the anharmonic transition probabilities are not available for solid neon.

VI. LIQUID NEON

A. Diffusion in Liquid Neon

Figure 6 shows the results of our NMR measurements of the diffusion of Ne^{21} in liquid neon. The diffusion coefficients were determined from measurements of the attenuation of spin echoes by an externally applied magnetic field gradient of known magnitude.[30] The gradient coils were calibrated in the manner described by Carr and Purcell and by calculation of the gradient assuming the magnet pole faces to be semi-infinite and including first image currents. The results of the two calibration methods agreed to within 2%. Most of our liquid-neon diffusion measurements were made using a gradient of about 2 G/cm.

The liquid-neon measurements were made at pressures between $0.02P_c$ and $0.1P_c$ (where P_c is the critical pressure, 25.9 atm[16]). The individual determinations of diffusion coefficients have an estimated error of ±10%. Over the range of the data, the coefficient of spin diffusion arising from the dipolar interaction among the Ne^{21} spins makes a negligible contribution to the observed diffusion rates.

A least-squares fit of the data of Fig. 6 to Eq.

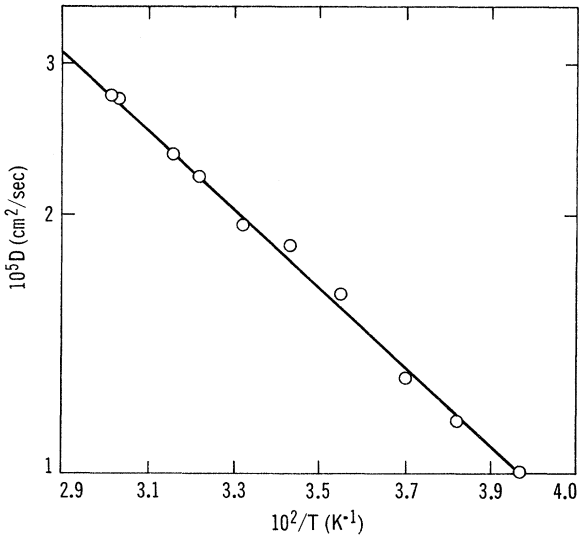

FIG. 6. Coefficient of self-diffusion in liquid neon. The solid line is a least-squares fit of an Arrhenius exponential to the data and corresponds to $E_D = 211$ cal/mole.

(4) yields the coefficients of self-diffusion for liquid neon,

$$D_0 = 6.6^{+2.1}_{-1.6} \times 10^{-4} \text{ cm}^2/\text{sec} ,$$

$$E_D = 211 \pm 15 \text{ cal/mole}.$$

The coefficients of atomic self-diffusion previously reported for liquid argon,[31] krypton,[15,31] and xenon[12,31] also have been found to obey Arrhenius relations. The variation of D with pressure[12,31] has been found to be small for pressures much less than the critical pressure.

Table III presents a comparison of the self-diffusion parameters E_D reported for the various rare-gas liquids. In krypton and xenon the NMR results are some 15% larger than the tracer values. The NMR values of E_D^*, reduced according to classical corresponding states, are nearly the same in the various rare gases and, in contrast with the behavior found for the solids (Fig. 4), any variation of the liquid E_D^* with Λ^* seems to be no more than 5% between neon and xenon.

TABLE III. Diffusion energies for rare-gas liquids.

	E_D	$E_D^* = E_D/\epsilon$
Ne (NMR)	211 cal/mole	2.89
Ar (tracer)	697 [a]	2.92
Kr (NMR)	926 [b]	2.83
(tracer)	800 [a]	2.45
Xe (NMR)	1400 [c]	3.04
(tracer)	1210 [a]	2.63

[a]Reference 31.
[b]Reference 15.
[c]Reference 12.

B. Spin-Lattice Relaxation in Liquid Neon

Spin-lattice relaxation times T_1 for Ne^{21} in liquid neon (Fig. 1) were measured between the melting point and 33.0 K at vapor pressures up to 4.3 atm. It is probable that the dominant relaxation mechanism is quadrupolar. Although the nuclear dipole-dipole interaction contributes appreciably to the Ne^{21} spin-relaxation rate in the hot solid near the melting point, the dipolar contribution is much reduced, upon melting, by the abrupt increase in the motional correlation frequency. In the liquid at the melting point the experimental conditions lie well into the extreme-narrowed regime ($\omega_0 \tau_c \ll 1$) and the calculated[8] dipolar T_{1D} is about 10^7 sec. Similarly, quadrupolar or dipolar relaxation via impurities should have been negligible for our clean neon samples.

The liquid T_1 data are shown, on an expanded scale, in Fig. 7. The dashed line indicates the temperature dependence reported above for the coefficient of self-diffusion in liquid neon. The solid line drawn through the T_1 data corresponds

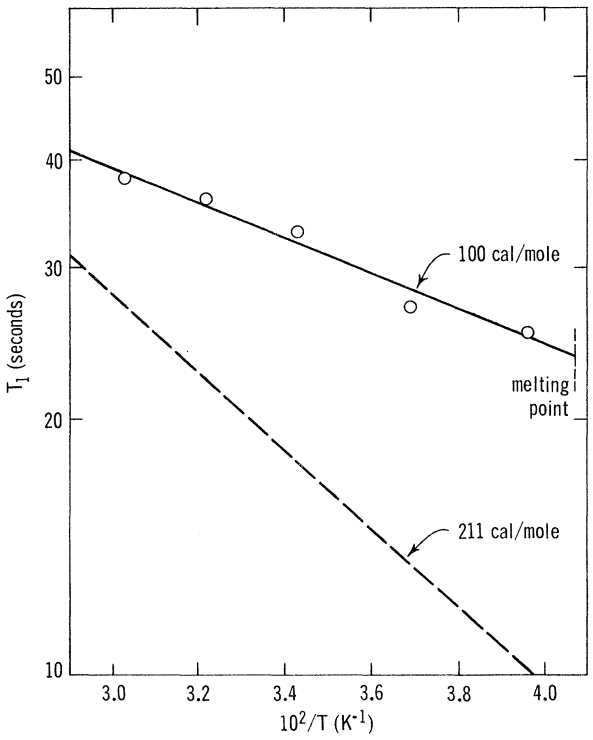

FIG. 7. Spin-lattice relaxation times for Ne^{21} in liquid neon. The dashed line indicates the temperature dependence observed for the coefficient of self-diffusion. The solid line is an exponential with an activation energy of 100 cal/mole.

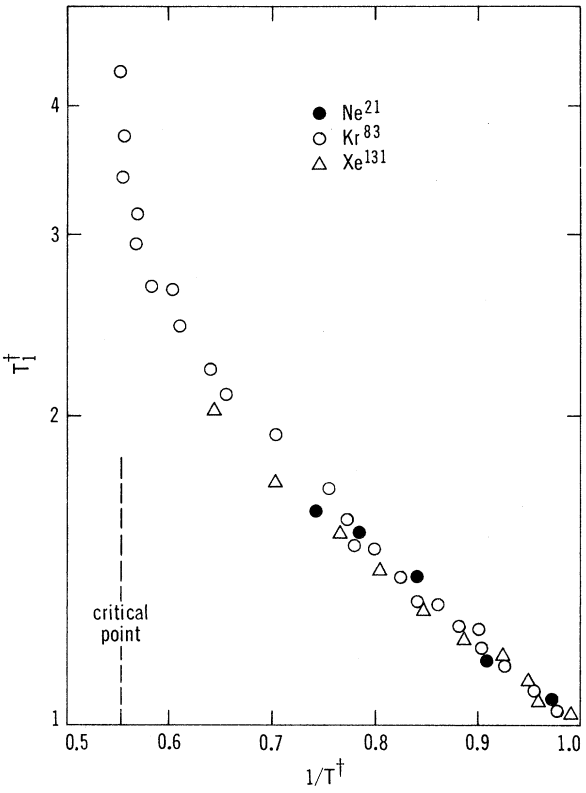

FIG. 8. Reduced spin-lattice relaxation times in liquid neon, krypton, and xenon. $T_1^\dagger$ is T_1 divided by its value at the triple point. $T^\dagger$ is the temperature divided by the triple-point temperature. The Xe^{131} data are from Ref. 26 and the Kr^{83} from Ref. 15.

to relaxation times proportional to $e^{-E/RT}$ with $E = 100$ cal/mole, a value somewhat less than one-half the energy parameter observed for self-diffusion, $E_D = 211$ cal/mole.

These results are similar to those reported over wider temperature intervals for Kr^{83} (spin $\frac{9}{2}$) in liquid krypton[15] and for Xe^{131} (spin $\frac{3}{2}$) in liquid xenon.[26] In each case, the temperature dependence of T_1 (if exponential) is about one-half that of D. However, T_1 for the Xe^{129} species (spin $\frac{1}{2}$) was found[12] to have the same temperature dependence as the xenon liquid diffusion coefficient. The Xe^{129} spin-lattice relaxation presumably arises from dipolar interaction with paramagnetic impurities, while the dominant T_1 processes for the Ne^{21}, Kr^{83}, and Xe^{131} species are quadrupolar.

Figure 8 shows the liquid T_1 data for Ne^{21}, Kr^{83}, and Xe^{131} in a reduced form, with $T_1^\dagger = T_1/(T_1)_{tr}$ and $T^\dagger = T/T_{tr}$, where T_{tr} is the triple-point temperature and $(T_1)_{tr}$ the value of T_1 at T_{tr}. There is a striking correspondence among the temperature dependences of T_1 in the three rare-gas liquids.

A single-particle diffusion model has proved to be inadequate for the description of the observed quadrupolar spin-lattice relaxation in the rare-gas liquids.[26] On the basis of such a model one considers relaxation via random time-dependent electric field gradients arising from exchange and van der Waals interactions between neighboring atoms. The assumption of an exponential correlation function then leads[26,32] to quadrupolar spin-lattice relaxation times proportional to D/ρ, in disagreement with the observations. The quadrupolar spin-lattice relaxation observed in rare-gas liquids is reminiscent of that reported in liquid metals and alloys.[33–35] It has been suggested[35,36] that the relaxation rates observed in liquid metals and alloys may contain appreciable quadrupolar contributions arising from quasicrystalline vibrations in the liquids. Warren[36] has derived an expression for the quadrupolar relaxation rate in monatomic liquids in terms of the dynamic liquid-structure factor determined from neutron-scattering experiments. Warren and Wernick[35] have estimated vibrational contributions R_{QV} to the quadrupolar relaxation rates R_Q in conducting liquid compounds by taking R_{QV} just above the melting temperature to be approximately the same as the observed R_Q in the solids just below T_m. They then find R_{QV} contributions between 20% and 50% of R_Q in their liquid samples.

For Ne^{21}, the quadrupolar T_1 in solid neon at the melting point is found (Fig. 5) to be 150 sec. The liquid T_1 at the melting point (Fig. 7) is 23.5 sec, and so an analysis similar to that of Warren and Wernick yields an approximately 16% vibrational contribution to the observed quadrupolar rate R_Q in liquid neon at the melting point. If one then extends the observed solid R_Q data (Fig. 5) smoothly into the temperature range of the liquid as a vibrational contribution R_{QV}, one can then examine the residual relaxation rate R' by the decomposition

$$1/T_1 = R_{QV} + R' .$$

For Ne^{21}, the resulting R' is an approximately exponential function of temperature with an activation energy about equal to the 211-cal/mole diffusion energy. Since the liquid density varies by only about 14% over the range of the Ne^{21} data, it may be that the residual R' can be interpreted in terms of a contribution from single-particle diffusion. A corresponding analysis yields similar results for liquid krypton and xenon.[15] The observed quadrupolar relaxation in the rare-gas liquids may exhibit both diffusional and vibrational contributions at temperatures not too far above the melting point.

VII. CONCLUSIONS

The Ne^{21} NMR line in solid neon exhibits dipolar and quadrupolar broadening. Motional narrowing of the resonance line as the temperature is in-

creased indicates a coefficient of self-diffusion in the solid which obeys an Arrhenius relation and corresponds well with the coefficients in other rare-gas solids, when a quantum-mechanical law of corresponding states is applied.

The spin-lattice relaxation of Ne^{21} in solid neon near the melting point exhibits a dipolar contribution arising from atomic self-diffusion. The principal T_1 mechanism in the solid, however, appears to be quadrupolar relaxation via the anharmonic Raman process.

The coefficient of atomic self-diffusion measured in liquid neon also exhibits an Arrhenius behavior and, as in the case of Kr^{83} in liquid krypton and Xe^{131} in liquid xenon, the quadrupolar T_1 in the liquid exhibits a temperature variation much slower than the ρ/D expected from single-particle diffusion models. If collective quasicrystalline vibrational modes do persist in liquid neon not too far above the melting point, then it is probable that they provide an appreciable contribution to the quadrupolar relaxation in the liquid.

---

*Based on a thesis submitted by R. H. in partial fulfillment of the requirements for the degree of Doctor of Philosophy in the Graduate School of Arts and Sciences, Washington University.

†Work supported by the U. S. Air Force Office of Scientific Research, the U. S. Army Research Office (Durham), and the NSF.

‡Present address: Department of Physics, Ohio State University, Columbus, Ohio.

[1]W. W. Warren, thesis (Washington University, 1965) (unpublished).

[2]G. L. Pollack, Rev. Mod. Phys. 36, 748 (1964).

[3]D. N. Batchelder, D. L. Losee, and R. O. Simmons, Phys. Rev. 162, 767 (1967).

[4]A. Shinichi and K. Eizo, J. Chem. Soc. Japan 55, 23 (1934).

[5]J. H. Van Vleck, Phys. Rev. 74, 1168 (1948).

[6]K. Kambe and J. K. Ollom, J. Phys. Soc. Japan 11, 50, (1956).

[7]W. W. Warren and R. E. Norberg, Phys. Rev. 154, 277 (1967).

[8]R. Kubo and K. Tomita, J. Phys. Soc. Japan 9, 888 (1954).

[9]P. W. Anderson and P. R. Weiss, Rev. Mod. Phys. 25, 269 (1953).

[10]M. Eisenstadt and A. G. Redfield, Phys. Rev. 132, 635 (1963).

[11]A. Abragam, *The Principles of Nuclear Magnetism* (Clarendon, Oxford, England, 1961), Chap. IV.

[12]W. M. Yen and R. E. Norberg, Phys. Rev. 131, 269 (1963).

[13]E. H. C. Parker, H. R. Glyde, and B. L. Smith, Phys. Rev. 176, 1107 (1968).

[14]A. V. Chadwick and J. A. Morrison, Phys. Rev. Letters 21, 1803 (1968); Phys. Rev. B 1, 2748 (1970).

[15]D. G. Cowgill and R. E. Norberg (unpublished).

[16]R. H. Beaumont, H. Chihara, and J. A. Morrison, Proc. Phys. Soc. (London) 78, 1462 (1961).

[17]G. L. Pollack, Phys. Rev. A 2, 38 (1970).

[18]E. Helfand and S. A. Rice, J. Chem. Phys. 32, 1642 (1960).

[19]N. Bernardes, Phys. Rev. 120, 807 (1960).

[20]T. G. Stoebe, T. O. Ogurtani, and R. A. Huggins, Phys. Rev. 132, 635 (1963).

[21]H. C. Torrey, Phys. Rev. 92, 262 (1953).

[22]H. A. Resing and H. C. Torrey, Phys. Rev. 131, 1102 (1963).

[23]J. Van Kranendonk, Physica 20, 781 (1954).

[24]J. Van Kranendonk and M. B. Walker, Phys. Rev. Letters 18, 701 (1967).

[25]J. Van Kranendonk and M. B. Walker, Can. J. Phys. 46, 2441 (1966).

[26]W. W. Warren, Jr. and R. E. Norberg, Phys. Rev. 148, 402 (1966).

[27]F. J. Adrian, Phys. Rev. 138, A403 (1965).

[28]P. Gombas, *Handbuch der Physik* (Springer-Verlag, Berlin, 1956), Vol. 36, p. 192.

[29]G. M. Grosof, P. Buck, W. Lichten, and I. I. Rabi, Phys. Rev. Letters 1, 214 (1958).

[30]H. Y. Carr and E. M. Purcell, Phys. Rev. 94, 630 (1954).

[31]J. Naghizadeh and S. A. Rice, J. Chem. Phys. 36, 2710 (1962).

[32]C. A. Sholl, Proc. Phys. Soc. (London) 91, 130 (1967).

[33]F. A. Rossini and W. D. Knight, Phys. Rev. 178, 641 (1969).

[34]W. W. Warren and W. G. Clark, Phys. Rev. 177, 600 (1969); 184, 606 (1969).

[35]W. W. Warren and J. H. Wernick, Phys. Rev. B 4, 1401 (1971).

[36]W. W. Warren, Bull. Am. Phys. Soc. 16, 338 (1971).